Rev. Mexicana Astron. Astrof., **24**, 99-107 (1992)

WIDE FIELD IMAGING OF THE STAR FORMING REGION LYNDS 1551

P.M. Garnavich, A. Noriega-Crespo, and P.J. Green[1]

Astronomy Department, University of Washington

Received 1991 September 25

RESUMEN

Hemos obtenido imágenes de la región de formación de estrellas L1551 usando filtros de banda angosta centrados en Hα y [S II] 6716/31. La mayoría de los nudos semi-estelares descubiertos recientemente por Graham and Heyer (1990) en sus imágenes en Hα + [N II] de esta zona, tiene también una fuerte emisión en [S II]. Tanto su estructura como su emisión sugiere que son objectos Herbig-Haro. El chorro opuesto de HH 30, a ~ 4 minutos de arco al noreste de IRS 5, se ve en las imágenes de Hα pero no en las de [S II]. Pensamos que el chorro opuesto de HH 30 puede estar interactuando con la cavidad de L1551 cerca de HH 102 la nebulosa de reflexión.

ABSTRACT

We have obtained images of the L1551 star forming region using narrow band filters centered on the Hα and [S II] 6717/31 emission lines. Many of the semi-stellar knots recently discovered in this zone by Graham and Heyer (1990) in their Hα + [N II] images have very strong [S II] emission. Their structure and emission suggest that these are Herbig-Haro objects. HH 30, at ~ 4 arcminutes NE of IRS 5, has a detectable counterjet in our Hα images, but is absent in the [S II] images. We suggest that the HH 30 counterjet may be interacting with the L1551 cavity near the reflection nebula in HH 102.

Key words: **HERBIG-HARO OBJECTS – NEBULAE-STRUCTURE – STARS-FORMATION**

I. INTRODUCTION

The star forming region Lynds 1551 (L1551) includes one of the most striking and (at a distance of ~ 160 pc) nearby examples of a molecular bipolar outflow (e.g., Snell, Loren, and Plambeck 1980; Bally and Lada 1983; Uchida and Shibata 1985; Strom *et al.* 1986; Uchida *et al.* 1987; Stocke *et al.* 1988). The region also contains several active young stellar objects (YSOs) all within a few arcminutes (see, e.g., Strom *et al.* 1986; Mundt *et al.* 1990). The bipolar outflow is powered by an embedded infrared source IRS 5 (Snell *et al.* 1980). From IRS 5 emanates a jet (Mundt and Fried 1983; Neckel and Staude 1987; Sarcander, Neckel, and Elsässer 1985), that may be responsible for the formation of Herbig-Haro (HH) objects HH 28 and HH 29 (Cudworth and Herbig 1979), and the HH 102 reflection nebula.

Among some of the YSOs in the immediate neighborhood of L1551 are the T Tauri stars XZ Tau and HL Tau, with their corresponding jet systems, as well as HH 30 and its jet (Mundt, Ray, and Bührke 1988; Mundt *et al.* 1990). The objects are so close together that complicated mutual interactions are likely to arise (e.g., Graham and Heyer 1990, hereafter GraHe).

Recently Rodríguez *et al.* (1989b) suggested the presence of two new sets of condensations in the L1551 region, based on their study of a red digitized Palomar Sky Survey image. One set forms an arc-like chain of ~ 7 objects that streams along with HH 29 and HH 28 (see Figure 1). A second set of condensations is at ~ 6 arcminutes NE of IRS 5. The morphology and location of these two groups of knots make them very likely HH object candidates (Rodríguez *et al.* 1989b). The existence of these condensations was confirmed by GraHe in their Hα + [N II] CCD survey of faint Hα emission-line stars in Taurus. Furthermore, a third previously unnoticed cluster of diffuse faint objects SW of HH 28 was found by GraHe. In this paper, we present

1. Visiting Astronomer, National Optical Observatory, which is operated by the AURA, Inc., under contract with NSF.

new [S II] narrow band images of the L1551 region, in which these new three set of condensations are clearly visible. Their strong [S II] intensity indeed suggests a shock-exciting process as responsible for their emission (see below).

Schwartz (1975) proposed that the emitted spectra observed in HH objects is produced in the recombination region behind a shock wave. Numerical models of the emitted spectrum in plane parallel shock waves (Dopita 1978; Raymond 1979; Raymond and Hartman 1984) and in bow shocks (Raga 1985; Hartigan, Raymond, and Hartmann 1987) support this idea. Based on this, HH objects are easily distinguishable from other emission nebulae, such as photoionized (H II) regions or reflection nebulae. The HH object spectrum is characterized by strong neutral emission lines in [O I] λ6300/63, [N I] λ5200 and [C I] λ9823/49, sometimes stronger than Hα (see e.g., Dopita 1978; Schwartz 1983). In practice, the recombination region is partially ionized, and therefore, free electrons interact with those elements with low ionization potentials, such as [Fe II] and [S II]. In the high excitation objects (e.g., HH 1 and HH 2) other emission lines such as [O III] λ4959/5007, [O II] λ3727/29 and [N II] λ6548/83 can be quite strong (see, e.g., Böhm 1983). It is this richness of low and high excitation lines, unlike e.g., the spectra of H II regions, that characterize the spectra of shock-excited regions.

Observationally, HH objects are particularly bright in [S II] λ6716/31, which can be comparable, or, as is the case in some low excitation HH objects (see, e.g., Böhm and Solf 1990), even stronger than Hα. This last characteristic, coupled with the high quantum efficiency of most CCDs in the 4000 - 7000 A range makes narrow band imaging in [S II] one of the best methods (along with spectroscopy) for identifying HH objects. The method has been successfully applied in the recent discoveries of HH objects (see, e.g., Reipurth 1989a,b,c; Ogura 1990; Ogura and Walsh 1991).

We present in this paper new narrow band CCD images in [S II], Hα, and the *R* and *I* broadbands. In §II we describe the observations and data reduction, and in §III we summarize our results.

II. THE OBSERVATIONS

a) *Observations and Data Reduction*

At Kitt Peak we obtained large area format CCD images of the L1551 region in the emission lines of [S II] and Hα. A focal reducer with the Tek1024 CCD provided an unvignetted image about 28′ in diameter at the 0.9-m telescope, with 2″ per pixel. On 10 December 1990, we obtained three 10 minute exposures of L1551 in [S II] (filter #812, λ_c = 6730 A, width = 86 A). For comparison purposes, we also observed the neighboring continuum (filter #1391, λ_c = 6619 A and width = 67 A) via three 6 minute exposures. All images were bias-subtracted and flat-fielded using IRAF, and the median of three images in each filter was performed to improve the signal-to-noise and to remove cosmic rays.

On 24 February 1991, with the same instrumental setup, we observed L1551 through cirrus in Hα (filter #811, λ_c = 6560 A and width = 89 A). Due to encroaching clouds, only 2 consecutive (15 minute) exposures could be obtained.

The region was also observed in September 1990 with the Manastash Ridge Observatory's (MRO) 0.8-m telescope, DAO focal reducer and "T-Bird" (Ford 1024) CCD. This combination provides a useful field of view 12′ in diameter. Images in broadband *R* and *I* as well as narrow band Hα, [N II] and continuum were obtained. The Hα filter also includes the [N II] 6548 A line, but the [N II] 6584 A filter reveals that the contamination to be minimal. The 20 A wide filters were centered at 6563, 6585 and 6629 A. The continuum was subtracted from the emission line images by scaling the continuum frame using stars in the field. Approximately ten stars were used to reduce errors caused by early (A-F type) stars. The raw fluxes for individual knots were measured using the IRAF POLYPHOT package with the same polygonal aperture applied to the [S II] and Hα minus continuum images. The flux ratios were all scaled such that [S II]/Hα = 0.33 for HH 29 (see below). The positions of the knots were obtained from a plate solution based on the Guide Star Catalog stars in the field (± 1 arcsecond), and have errors of the order of ± 3 arcseconds.

b) *Calibration of the Narrow Bandpass Images*

The ratio of [S II] (6717+6731) to Hα was measured for the bright emission features HH 28 and HH 29. These objects were then used as secondary standards to estimate the ratio for the other emission knots in the L1551 region. Calibrating the integrated line ratio using slit spectra was undesirable because the slits generally select only a small area of the emission knot. Besides, a literature search provided no reliable [S II]/Hα ratios obtained from spectra of HH 28 or HH 29 (but see Strom, Grasdalen, and Strom 1974).

The L1551 complex was imaged in five narrow bandpasses at MRO in August, 1991. Two filters were centered on Hα and had widths of 20 A and 10 A. The remaining filters consisted of [N II] (FWHM = 20 A), [S II] (FWHM = 67 A) and continuum (λ_c = 6629, FWHM = 20 A). A spectrophotometric continuum standard and the planetary nebula Me1 -1 were also observed in these filters. Me1-1 was chosen as a calibrator because its [S II]/Hα ratio is large for a planetary nebula and because it has a nearly stellar appearance.

After removing the continuum contribution, the line strengths of Me1-1 (Aller and Keyes 1987) were used to estimate the relative sensitivities of the bandpasses at the wavelengths of the emission lines. The two Hα and the [N II] filters were helpful in estimating the contamination of λ6563 by λλ6584 and 6548 in the planetary nebula. To avoid errors caused by velocity differences and broad lines in the HH-objects, only the 20 A Hα filter was used in the final calibration. The [S II]/Hα ratio obtained for both HH 28 and HH 29 was 0.33±0.03

c) *The Central and NE Region of L1551*

A detailed description of the central L1551 region has been given by GraHe. The region contains two highly obscured infrared sources, L1551 NE (Emerson *et al.* 1984) and IRS 5 (Strom, Strom, and Vrba 1976). The IRS 5 source drives the molecular bipolar outflow (Snell *et al.* 1980) and seems to be responsible for optically bright features such as HH 28, HH 29 and HH 102 (Strom *et al.* 1974; Cudworth and Herbig 1979).

In Table 1, we present a list of objects previously identified by Strom *et al.* (1974) and GraHe in the central zone of L1551. We give the position for each object in the second and third columns. The fourth column lists the Hα + [S II] 6717/31 intensity, normalized to that of HH 29 (= 1.0), as a relative measurement of brightness. The fifth column contains the [S II]/Hα ratio scaled to the HH 29 value (= 0.33) as an estimate of excitation (Böhm 1983). In the last column, we list distances in arcminutes with respect to the IRS 5 source. Table 2 is a similar list of approximately 20 additional objects that we have identified in our [S II] and Hα frames (see Figures 1 and 2).

About 8 objects are in the immediate neighborhood of HH 102 and HH 29 (see Figure 2). One of the interesting features of this group is the "knot #3", which seems to be aligned with the HH 30 counterjet (see §IIc). The chain of objects noted by Rodríguez *et al.* (1989b) along HH 28 and HH 29 is clearly visible in our [S II] image without the continuum subtracted (see Figure 2). The three most westerly of the seven condensations of this group are due to reflection. "Knot #2" is very strong in [S II] and "knot #5" is only visible in Hα. The different emission of "knot #2" and "knot # 5" may indicate a more complex process for the origin of the knots than one simply arising from Kelvin-Helmholtz instabilities in the flow (Rodríguez *et al.* 1989b). Another possibility is that knots are the result of internal shocks (internal working surfaces) produced by a time-varying stellar jet (Raga *et al.* 1990; Raga and Noriega-Crespo 1992). In this case, the emission of the knot will depend on the characteristics of the internal shock (Noriega-Crespo 1992).

The new cluster of diffuse objects SW of HH 28

TABLE 1

L1551 HH OBJECTS

Emission Object[a]	R.A. (1950)	Dec. (1950)	Hα+[S II] (HH 29=1.0)	[S II]/Hα (HH 29=0.33)	$Dist_{IRS5}$ arcmin
HH 28 = SH 211	$4^h28^m13.0^s$	+17°56′56″	0.57	0.35	3.9
HH 29 = SH 207	4 28 33.2	+17 59 59	1.00	0.33	1.2
SH 219/220	4 28 36.1	+18 00 30	0.26	0.09	0.7
SH 229	4 28 20.3	+17 57 38	0.26	0.50	3.0
GH 1	4 28 00.8	+17 52 42	0.13	2.63	6.4
GH 2	4 28 04.2	+17 57 10	0.27	0.76	4.7
GH 3	4 28 04.8	+17 57 37	0.05	0.39	4.6
GH 4	4 28 07.4	+17 57 36	0.20	0.62	4.3
GH 5	4 28 07.4	+17 57 13	0.14	1.58	4.4
GH 6	4 28 08.1	+17 56 30	0.08	1.18	4.5
GH 7	4 28 10.3	+17 57 24	0.14	2.25	4.1
GH 8 = SH 217	4 28 12.1	+17 57 06	0.46	1.03	4.0
GH 9	4 29 04.9	+18 05 46	0.18	0.65	3.5
GH 10W	4 29 06.1	+18 05 13	0.11	0.85	3.5
GH 10E	4 29 07.1	+18 05 03	0.28	1.02	3.6

a. SH = Stocke *et al.* 1988; GH = Graham and Heyer 1990.

TABLE 2

ADDITIONAL EMISSION OBJECTS IN L1551

Emission Object[a]	R.A. (1950)	Dec. (1950)	Hα+[S II] (HH 29=1.0)	[S II]/Hα (HH 29=0.33)	Comments
1	$4^h28^m33.1^s$	+18°00′ 31″	0.08	0.84	Rodr. chain
2	4 28 31.3	+17 59 31	0.18	1.01	Rodr. chain
3A = SH 214	4 28 29.5	+18 01 24	0.30	0.34	HH 30 jet?
3B	4 28 29.1	+18 01 08	0.26	0.43	HH 30 jet?
3C	4 28 28.8	+18 00 49	0.43	0.54	HH 30 jet?
4A = SH 212	4 28 25.1	+18 01 00	0.35	0.49	...
4B	4 28 24.8	+18 00 34	0.67	0.56	...
4C = SH 210	4 28 23.4	+18 00 09	0.70	1.27	...
4D	4 28 24.6	+17 59 52	0.61	0.43	...
4E	4 28 24.9	+17 59 34	0.80	0.45	...
4F	4 28 24.6	+17 59 15	0.47	0.32	...
4G = SH 208/9	4 28 26.3	+17 59 59	0.72	0.32	...
4H	4 28 26.1	+18 00 22	0.17	0.24	...
5	4 28 28.7	+17 58 58	0.16	<0.09	Rodr. chain
6	4 28 26.5	+17 58 54	0.09	<0.09	...
7A	4 28 23.6	+17 58 49	0.32	0.48	...
8	4 28 23.6	+17 58 32	0.23	0.75	...
9	4 28 22.4	+17 58 18	0.19	1.13	...
10	4 28 19.3	+17 58 10	0.40	0.56	...
11	4 28 17.9	+17 57 35	0.15	0.91	...
12	4 28 14.7	+17 57 39	0.20	1.23	near HH 28
13	4 28 14.3	+17 57 02	0.33	0.54	near HH 28
14	4 28 13.0	+17 57 29	0.23	1.16	near HH 28
15	4 28 11.4	+17 57 39	0.13	1.07	near HH 28
16	4 28 06.5	+17 56 56	0.15	1.35	near HH 28
17	4 28 07.0	+17 54 17	0.27	0.87	NE of IRS 5
18	4 29 07.1	+18 06 13	0.10	1.24	NE of IRS 5
19	4 29 06.7	+18 05 48	0.09	1.92	NE of IRS 5
20	4 29 06.7	+18 05 31	0.13	1.64	NE of IRS 5
21	4 29 08.1	+18 04 47	0.17	0.76	NE of IRS 5
22	4 29 05.8	+18 04 11	0.10	0.87	NE of IRS 5
23	4 29 03.0	+18 05 05	0.15	0.91	NE of IRS 5
24	4 28 58.2	+18 10 28	0.42	<0.09	HH 30 jet
25	4 28 21.0	+18 05 35	0.07	>1.78	...

a. SH = Stocke *et al.* 1988; Rodr. chain = Rodríguez *et al.* 1989.

detected by GraHe in their Hα + [N II] survey is very intense in our [S II] images. Unlike the other two bright HH objects, HH 28 and HH 29, the diffuse objects are not aligned with the IRS 5 source, and they seem to be spreading out at the end of the cavity (see, e.g., Figure 2, knots GH 2, GH 5 and GH 7). Since hydrodynamic stellar jets do not bend, this distribution of knots is difficult to explain with current models (see, e.g., Raga 1988; Hartigan 1989; Blondin, Fryxell, and Königl 1990; Tenorio-Tagle and Różyczka 1991). More speculative models of the L1551 jet include precession (Lightfoot 1987; Raga 1991), or a twisted magnetic field configuration (Uchida and Shibata 1987).

Most of these diffuse emission objects have very large [S II]/Hα ratios (≥ 2) when compared to HH 28 or HH 29 (see Table 1). If the emission from the knots is shock-excited, then large ratios indicate an extremely low excitation or shock velocities (see,

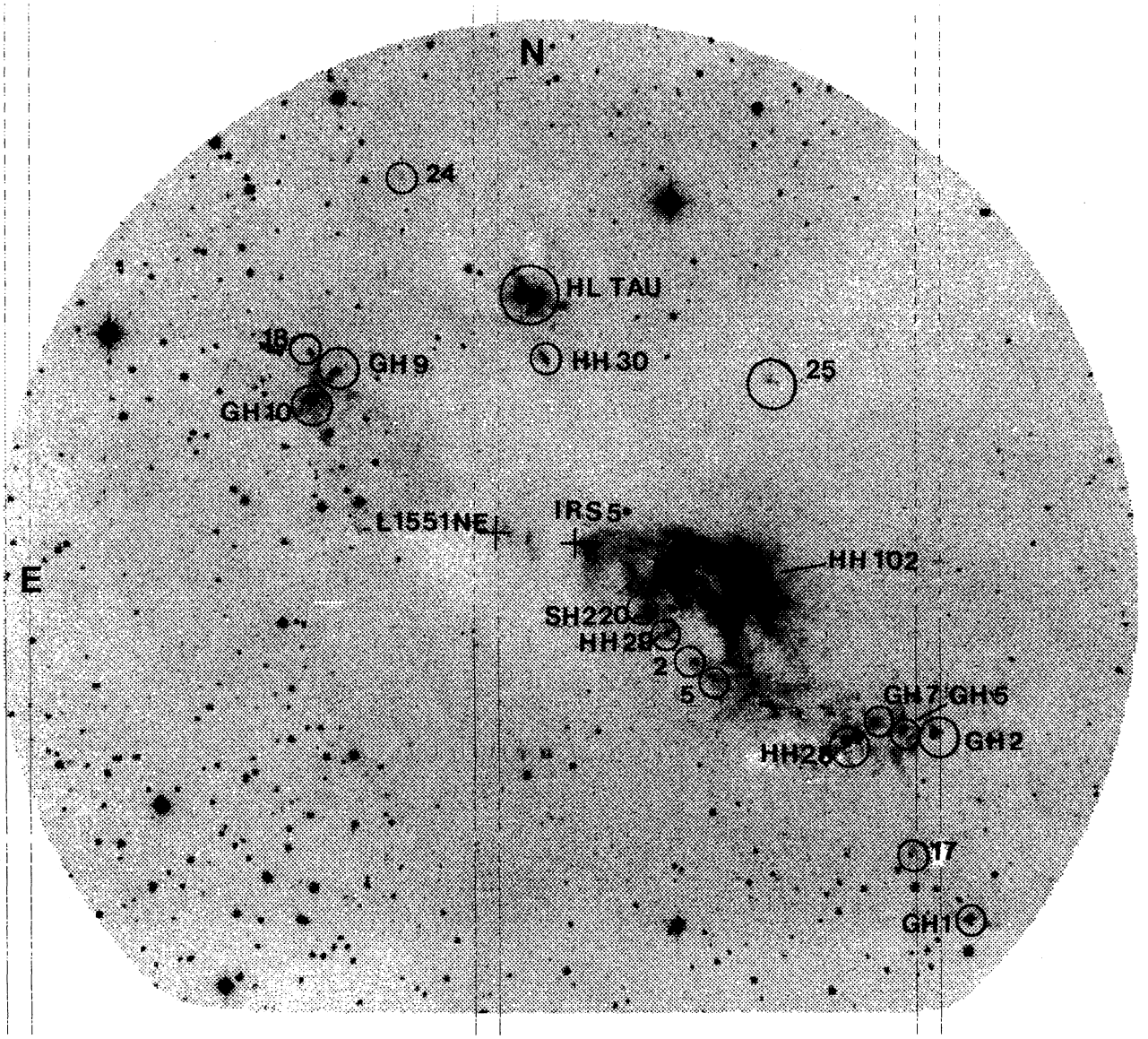

Fig. 2. CCD image in [S II] 6717/31 of L1551. The positions of the two infrared sources (IRS 5 and L1551 NE), HH 28, HH 29, HH 102, as well as several of the Hα objects observed by Graham and Heyer (1990) are marked. The continuum has not been removed. The lines across the image are an artifact from the data reduction package IRAF.

e.g., Böhm 1983). Plane parallel shock models (Hartigan *et al.* 1987), for instance, predict [S II] 6717+31/Hα ratio ~ 2.3 for a shock velocity of 20 km s^{-1}, with equilibrium preionization and a gas density of 100 cm^{-3}. Fully preionized models with similar density and velocity predict a ratio of ~ 0.3. Kinematical one-dimensional bow shock models (Hartigan *et al.* 1987) predict a smaller ratio, ~ 1.2, for comparable shock velocity and gas density (30 km $s^{-1}$and 300 cm^{-3}).

In the NE region of L1551, about 6 arcminutes from the IR source L1551 NE, there is a group of 3 or 4 "fuzzy knots", identified by GraHe as possible HH object candidates. These knots are clearly seen in our [S II] images (see Figure 3), and have relatively low excitation (see Tables 1 and 2). For example, the GH 9, GH 10W and GH 10E knots have [S II]/Hα ratios of ~ 0.65, 1.02 and 0.85, respectively (for HH 29 = 0.33), while knots "#18", "#19" and "#20" have even larger ratios, ~ 1.44, 1.92 and 1.64, respectively.

The NE knots, as indicated by GraHe, appear to be related to the L1551 NE source rather than to IRS 5. The knots seem to lie at the boundary of the blue-shifted lobe of the newly detected molecular bipolar outflow in L1551 by Moriarty-Schieven and

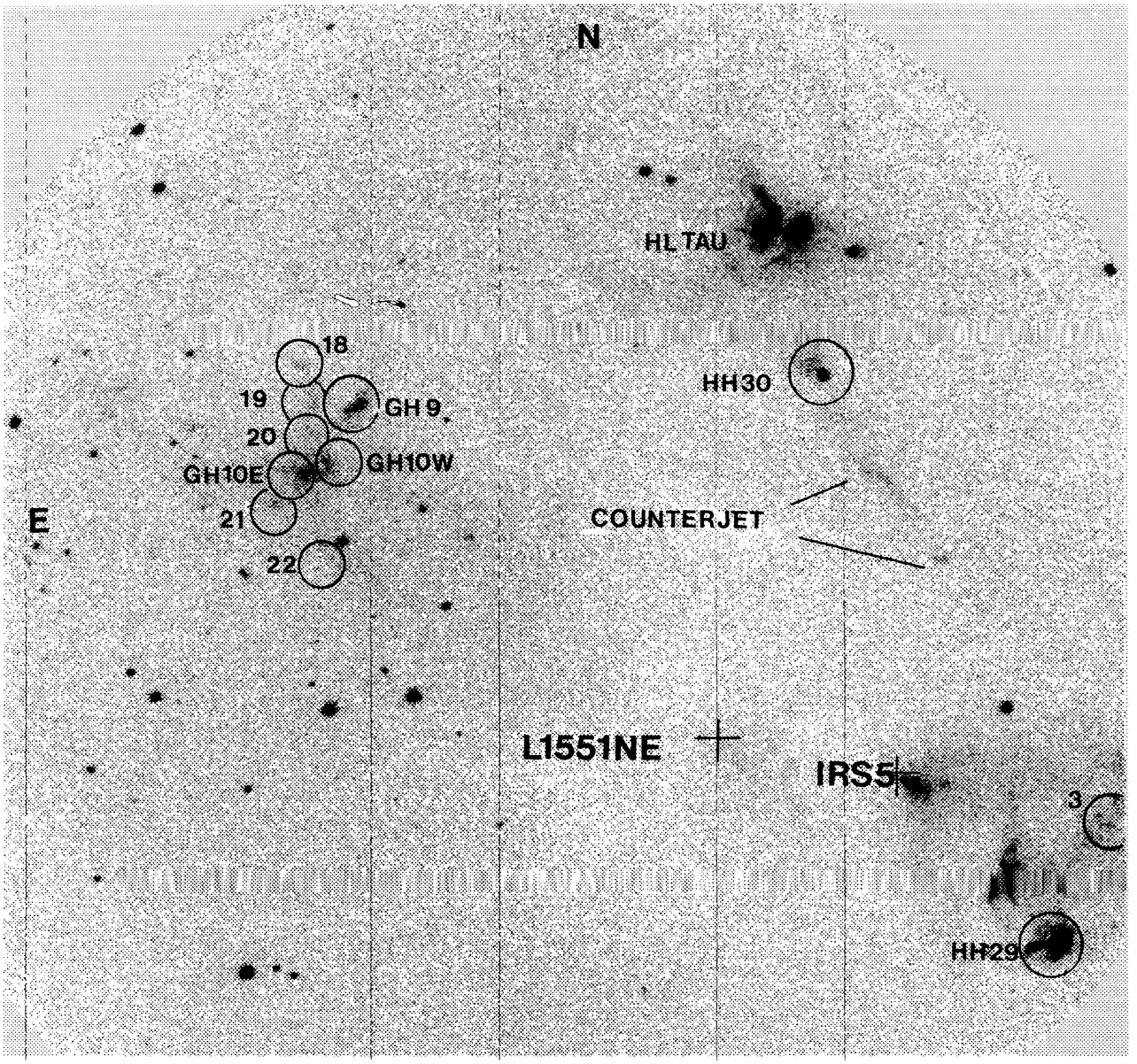

Fig. 3. Hα frame of the L1551 central region (with the continuum subtracted). The position of HH 30 (at the upper left) and several of the new "fuzzy" objects are marked (see text for details). Notice that knot #3 (below the HH 102 nebula) seems to be aligned with the HH 30 counterjet. Positions for the knots are in Tables 1 and 2.

Wannier (1991). This second outflow could also be driven by L1551 NE (Moriarty-Schieven and Wannier 1991; Pound and Bally 1991). Radial velocities and proper motions of the knots, however, are required to confirm such a scenario.

c) *The HH 30 Jet and Counterjet System*

The HH 30 system lies about 4 arcminutes north of IRS 5. Further north about 2 arcminutes lie the YSOs: XZ Tau, HL Tau and VLA 1, with their respective jet systems. The region has been extensively studied (see, e.g., Strom *et al.* 1974; Mundt *et al.* 1988; Mundt *et al.* 1990), and as pointed out by GraHe, the proximity of these jets give rise to complex mutual interactions. In Figure 4, we show our Hα continuum-subtracted image of the central L1551 region including HH 30 and its counterjet. The absence of HH 102 reflection nebula attests to the quality of the image subtraction. We have marked the positions of

essentially all the Hα knots above background in Figure 4, including those identified by Stocke *et al.* (1988) and GraHe (see also Table 2).

The HH 30 counterjet is faint, relatively broad and ragged in our Hα images. Its emission can be traced nearly up to the HH 102 reflection nebula. The counterjet, however, is not visible in any of our [S II] images, which is somewhat surprising since in most models of emission from stellar jets, the low and medium excitation lines (i.e., e.g., [S II] 6717/31, [N II] 6548/83, [O I] 6300/63 and [C I] 9849) can be as strong or stronger than Hα (Raga 1988).

It would seem, at least morphologically, that "knot #3", near the inner edge of HH 102, arises from the interaction of the HH 30 counterjet and material in the cavity (see Figure 4). This idea is partially supported by the difference between the

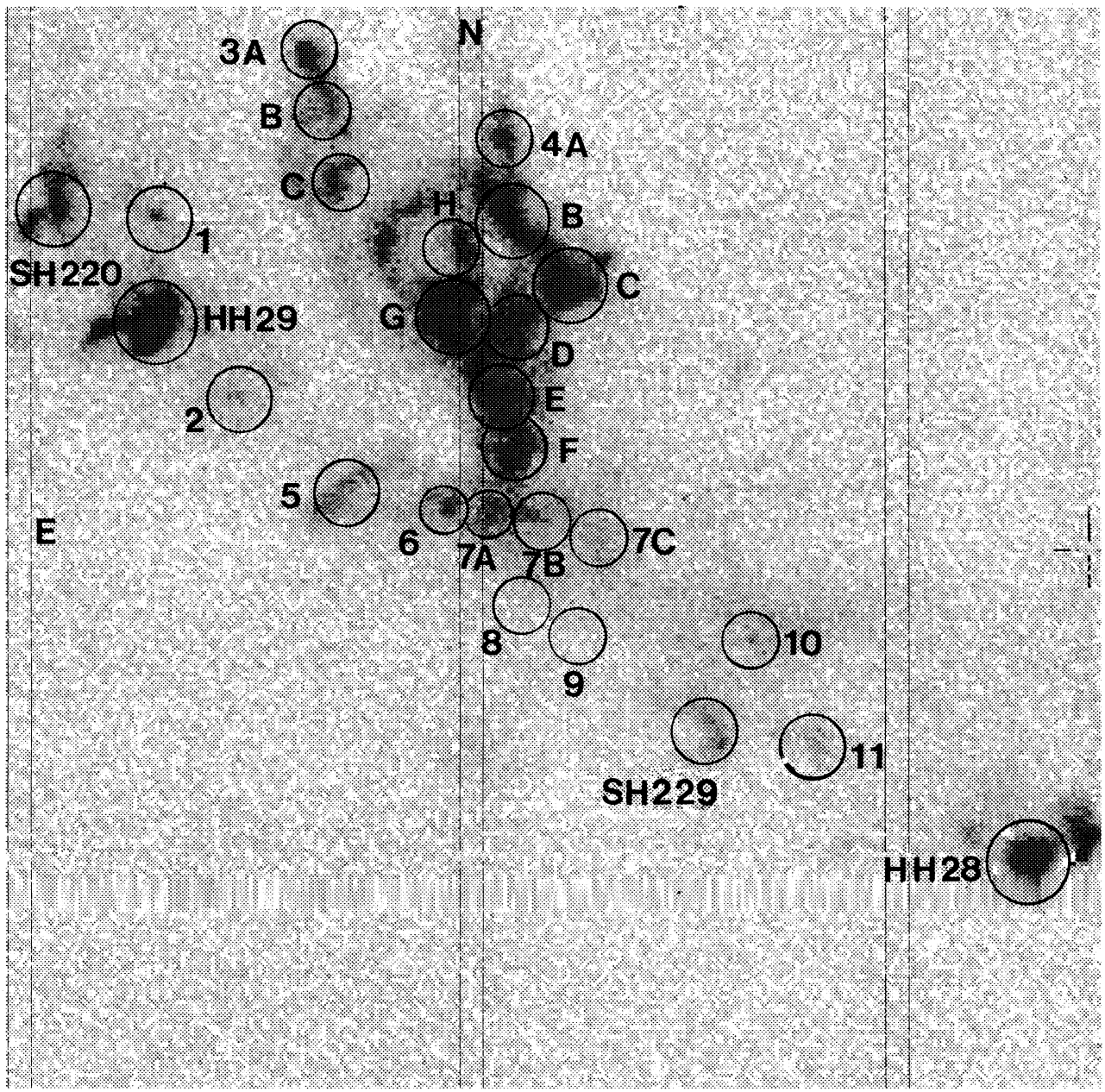

Fig. 4. Hα image taken at MRO (with the continuum subtracted) showing the knots in the central region of L1551. The positions for knots #8 and #9 are marked, although these are only visible in [S II]. The postions for the knots are in Tables 1 and 2.

radial velocities and excitation of "knot # 3" and the rest of the nearby knots (see below). The relatively short distance between HH 30 and "knot #3" (~ 4 arcminutes or ~ 0.2 pc at 160 pc) is another contributing factor. The condensations HH 28 (SH 211), HH 29 (SH 207), GH 8 (SH 217) and SH 229, presumably aligned with and excited by IRS 5, have maximum radial velocities of ~ −160 km s^{-1}(Stocke *et al.* 1988, Fig. 8 and Table 4). The knots close to HH 102 (i.e., SH 210 and SH 214 = #3), on the other hand, have radial velocities between ~ −15 and ~ −30 km s^{-1}. These latter values are very uncertain (Stocke *et al.* 1988), but definitely smaller than for the knots excited by IRS 5. The SH 210 and "#3" condensations (unlike the diffuse HH objects) display a higher excitation (0.34 - 0.54) similar to that of the shock-excited HH 29 and HH 28.

The radial velocities associated with the HH 30 the jet system have been measured by Mundt *et al.* (1990). They found that both jet and counterjet have similar and small radial velocities (15 ± 10 km s^{-1}), setting the system essentially in the plane of the sky (for an HH 30 jet velocity of ~ 400 km s^{-1}). The data are consistent with, the HH 30 bipolar jet, "knot #3" and knot SH 210 to be essentially in the plane of the sky. HH 30 counterjet, given their relative proximity, could then be responsible for the excitation of these knots.

Finally, we found two faint, small and distant condensations (see Figure 2), "knot #24" and "knot #25", that have been unnoticed in previous studies (e.g., Stocke *et al.* 1988; GraHe; Mundt *et al.* 1990). The "knot #24" may be aligned with the HH 30 jet, and has a relatively small [S II]/Hα ratio (< 0.09). The "knot #25" lies at ~ 4 arcminutes NW of IRS 5 and it does not seem to be related to any of the nearby YSOs. This knot, which appears in our three [S II] frames, but not in the three off band images, has a large [S II]/Hα ratio (> 1.8)

III. SUMMARY

We present new CCD images of the L1551 star forming region centered on the [S II] 6717/31 and Hα wavelengths to investigate the nature of the new knots discovered by GraHe. For all the new knots, we measured their positions, [SII]+Hα fluxes and [S II]/Hα line ratios, relative to HH 29 (Tables 1 and 2). We find that most of the new fuzzy knots are bright in [S II], which strongly suggests that they are Herbig-Haro objects (Schwartz 1975). Most of the new HH objects SW of HH 28 and some NE of IRS 5, have large [S II]/Hα ratios ($\geq$ 1.0), indicating very low ionization. The knots GH 1 and GH 7, for instance, have ratios of $\geq$ 2.25. For comparison, the [S II]/Hα ratios for some of the "classical" low excitation HH objects are ~ 3.7, ~ 1.5 and ~ 1.5 for HH 7, HH 11 and HH 43C, respectively (Böhm and Solf 1990). To obtain such large values, plane parallel shock models require low velocities ($\leq$ 30 km s^{-1}) and high preionization for typical preshock densities of 100 - 300 cm^{-3}(Hartigan *et al.* 1987, Noriega-Crespo 1992).

The new cluster of HH objects NE of IRS 5 seems to be aligned with the infrared source L1551 NE. The presence of a second molecular bipolar outflow in the L1551 (e.g., Moriarty-Schieven and Wannier 1991), covering the same area of these new knots with its blue-shifted lobe, strongly suggests L1551 NE to be the responsible driving source. Spectroscopy of these new HH objects may resolve the issue.

The new condensations SW of HH 28 show a different excitation and alignment than the chain of knots along HH 29 and HH 28, and may not have been produced by a steady stellar jet. A time-dependent stellar jet, coupled with another mechanism such as a precession (Lightfoot 1987) or a specific magnetic field configuration may be necessary to explain their structures (Uchida and Shibata 1987). Without the complete kinematical and dynamical data of these objects, both scenarios remain highly speculative.

The detection of the HH 30 counterjet in Hα but not in [S II], as well as its possible interaction with the HH 102 reflection nebula, deserve further attention. The HH 30 jet is observed in [S II] with a length of ~ 3 arcminutes (see, e.g. Mundt *et al.* 1990, Fig. 1). The absence of the counterjet in [S II] may indicate different physical conditions there. The lack of one of the stellar jet components of a bipolar outflow, as in the case of HH 34 (see, e.g., Bührke, Mundt, and Ray 1988) or HH 1/2 (see, e.g., Solf and Böhm 1991), is explained in terms of a somewhat higher extinction in the direction of the "missing jet". If the jet system is not exactly in the plane of the sky, then one of the components would move deeper into the obscuring molecular cloud, while the opposite jet would break through the boundary of the cloud, becoming visible.

A similar explanation is plausible for the HH 30 counterjet, which could be invisible in our [S II] images due to a higher attenuation. Light scattering by dust particles in the surrounding medium, however, permit us to observe the faint, ragged counterjet in Hα. Theoretical and observational arguments support the importance of light scattering as a cause of the broadening and asymmetry of the line profiles along stellar jets (see, e.g., Calvet *et al.* 1992), as well as in their working surfaces (see, e.g., Noriega-Crespo *et al.* 1991). If the extent of the HH 30 counterjet is similar to that of the jet, then L1551 and HH 30 are likely to be interacting. Further spectroscopic observations are needed to decide this point.

It is a pleasure to thank K.-H. Böhm, A. Raga and L.F. Rodríguez for useful conversations. We thank E. Carder of KPNO and P. Hodge for loaning us the filters, and N. King for help with the observations. We thank the anonymous referee for her/his comments. ANC's research has been funded by the NSF grant 89-18458.

REFERENCES

Aller, L., & Keyes, C.D. 1987, ApJS, 65, 405
Bally, J., & Lada, C. 1983, ApJ, 265, 824
Blondin, J.M., Fryxell, B.A. & Königl, A. 1990, ApJ, 360, 370
Böhm, K.H. 1983, RevMexAA, 7, 55
Böhm, K.H., & Solf, J. 1990, ApJ, 348, 297
Bührke, T., Mundt, R., & Ray, T.P. 1988, A&A, 200, 99
Calvet, N., Cantó, J., Raga, A.C., Lizano, S., & Binette, L. 1992, in preparation
Cudworth, K.M. & Herbig, G. 1979, AJ, 548
Dopita, M.A. 1978, ApJS, 37, 117
Emerson, J.P., Harris, S., Jennings, R.E., Beichmann, C.A., Baud, B., Beintema, D.A., Marsden, P.L., & Wesselius, P.R. 1984, ApJ, 278, L49
Graham, J.A., & Heyer, M.H., 1990, PASP, 102, 972 (GraHe)
Hartigan, P. 1989, ApJ, 339, 987
Hartigan, P., Raymond, J.C., & Hartmann, L. 1987, ApJ, 316, 323
Lightfoot, J.F. 1987 in IAU Symposium 122, Circumstellar Matter, eds. I. Appenzeller and C. Jordan (Dordrecht:Reidel) p. 75
Moriarty-Schieven, G.H., & Wannier, P.G. 1991, ApJ, 373, L23
Mundt, R., & Fried, J.W. 1983, ApJ, 274, L83
Mundt, R., Ray, T., & Bürkhe, T. 1988, ApJ, 333, L69
Mundt, R., Ray, T.P., Bührke, T., Raga, A.C., & Solf, J. 1990, A&A 232, 37
Neckel, T., & Staude, H.J. 1987, ApJ, 322, L27
Noriega-Crespo, A. 1992, in preparation
Noriega-Crespo, A., Calvet, N., & Böhm, K.H. 1991, ApJ, 379, 676
Ogura, K. 1990, PASP, 102, 1366
Ogura, K., & Walsh, J.R. 1991, AJ, 101, 185
Pound, M.W., & Bally, J. 1991, ApJ, 383, 705
Raga, A.C. 1985, Ph.D. Thesis, University of Washington
____. 1988, ApJ, 335, 820
Raga, A.C., Cantó, J., Binette, L., & Calvet, N. 1990, ApJ, 364, 651
Raga, A.C. & Noriega-Crespo, A. 1992, RevMexAA, 24, 9
Raga, A.C. 1991, private communication
Raymond J.C. 1979, ApJS, 39, 1
Raymond, J.C. & Hartmann, L. 1984, ApJ, 276, 560
Reipurth, B. 1989a in ESO Workshop on Low Mass Star Formation and Pre-Main Sequence Objects, ed. Bo Reipurth, p. 247
____. 1989b, A&A, 220, 249
____. 1989c, Nature, 340, 42
Rodríguez, L.F., Cantó, J., Moreno, M.A., & López, J.A. 1989b, RevMexAA, 17, 111
Sarcander, M., Neckel, T., & Elsässer 1985, ApJ, 288, L51
Schwartz, R.D. 1975, ApJ, 195, 631
____.1983, RevMexAA, 7, 27
Snell, R.L., Loren, R.B., & Plambeck, R.L. 1980, ApJ, 239, L17
Solf, J., & Böhm, K.H., 1991, ApJ, 375, 618
Stocke, J.T., Hartigan, P.M., Strom, S.E., Strom, K.M., Anderson, E.R., Hartmann, L.W., & Keynon, S.J. 1988, ApJS, 68, 229
Strom, S.E., Grasdalen, G.L., & Strom, K.M. 1974, ApJ, 191, 111
Strom, K.M., Strom, S.E., & Vrba F.J. 1976, AJ, 81, 321
Strom, K.M., Strom, S.E., Wolf, S., Morgan, J., & Wenz, M. 1986, ApJS, 62, 39
Tenorio-Tagle, G. & Różyczka, M. 1991, A&A, 245, 616
Uchida, Y., Kaifu, N., Shibata, K., Hayashi, S.S., Hasegawa, T., & Hamatake, H. 1987, PASJ, 39, 907
Uchida, Y., & Shibata, K. 1985, PASJ, 37, 515
____. 1987 in IAU Symposium 122, Circumstellar Matter, eds. I. Appenzeller and C. Jordan (Dordrecht:Reidel), p. 77

Peter M. Garnavich, Paul J. Green, and Alberto Noriega-Crespo: Astronomy Department FM-20, University of Washington, Seattle, WA 98195, USA.

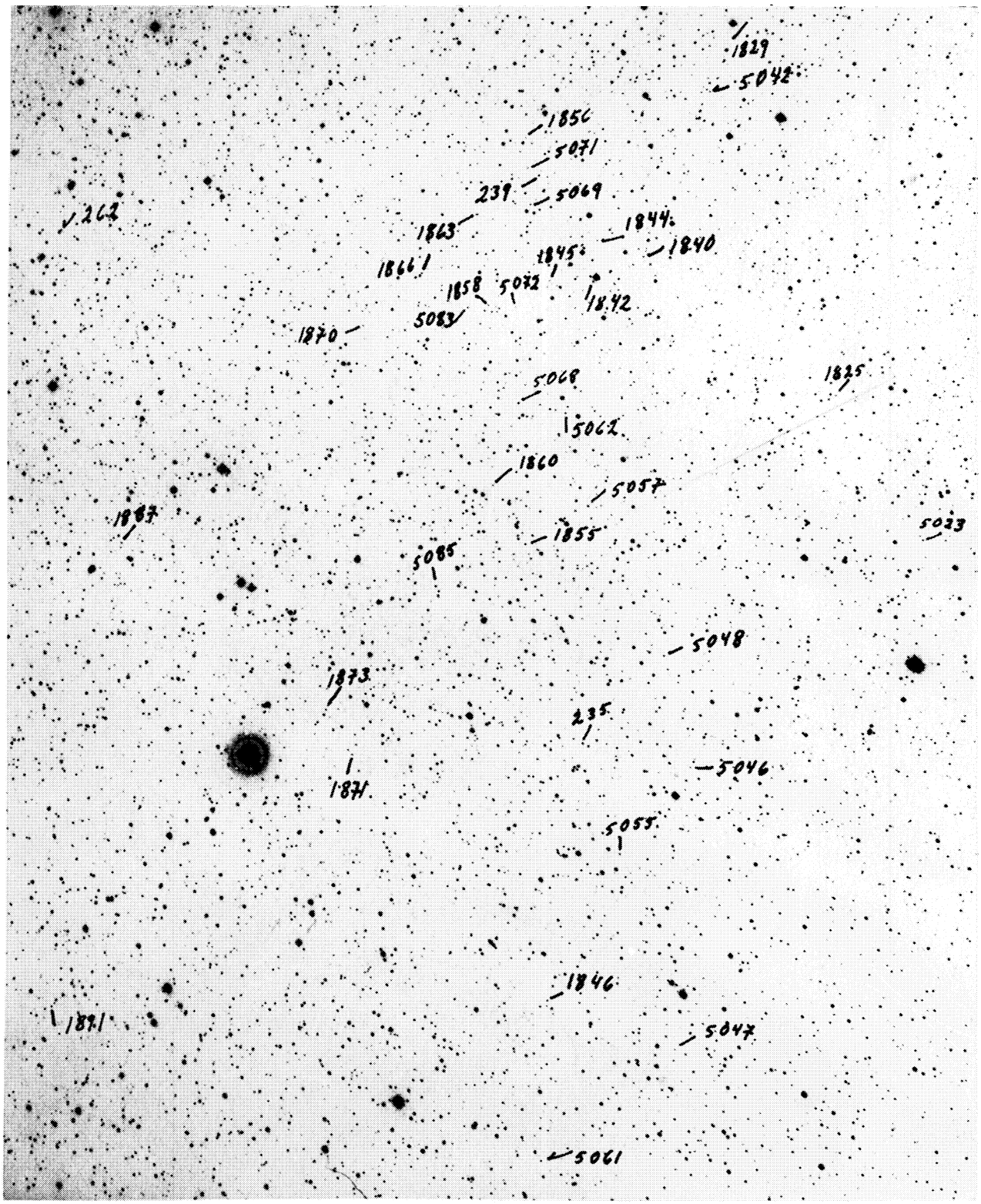

Fig. 1. Identification charts.

CHAVIRA (See page 139)